Layover and shadow detection based on distributed spaceborne single-baseline InSAR

Zou Huanxin[1], Cai Bin[2], Fan Changzhou[2] and Ren Yun[1]
[1] UWB Lab, School of Electronic Science and Technology, National University of Defense Technology, Changsha, Hunan, China
[2] Telecommunication Engineering Institute, Air Force Engineering University, Xi'an, Shanxi, China

E-mail:[1] hxzou2008@163.com
[2] Caibin2004@yahoo.com.cn

Abstract: Distributed spaceborne single-baseline InSAR is an effective technique to get high quality Digital Elevation Model. Layover and Shadow are ubiquitous phenomenon in SAR images because of geometric relation of SAR imaging. In the signal processing of single-baseline InSAR, the phase singularity of Layover and Shadow leads to the phase difficult to filtering and unwrapping. This paper analyzed the geometric and signal model of the Layover and Shadow fields. Based on the interferometric signal autocorrelation matrix, the paper proposed the signal number estimation method based on information theoretic criteria, to distinguish Layover and Shadow from normal InSAR fields. The effectiveness and practicability of the method proposed in the paper are validated in the simulation experiments and theoretical analysis.

1. Introduction

Distributed spaceborne single-baseline InSAR is an effective technique to get high quality Digital Elevation Model. Layover and Shadow are ubiquitous phenomenon in SAR images because of geometric relation of SAR imaging. The shadow and layover percentage in the SAR images are also exploited to optimize the baseline and incidence angle design of the InSAR system [1].

Traditionally, the coherence of the two SAR images or the images' intensity are exploited to identify the shadow and layover regions[2]. M. Eineder[2] reconstructs the shadow regions phase to improve DEM reconstruction using these ordinary isolation method. However, coherence or SAR intensity information are not sufficient to discriminate the areas that are dark and decorrelated because of other reasons, such as smooth surface like lakes or roads, and sand deserts[2]. F. Gini proposed a new layover detection method based on Capon, Root-MUSIC, APES and RELAX in the multibaseline InSAR system[3]. M. Eineder proposed a maximum-likelihood estimator to simultaneously unwrap, geocode, and fuse SAR interferograms from different viewing geometries into one digital elevation model[4].

This paper analyzed the geometric and signal model of the Layover and Shadow fields with the single-baseline InSAR system. Based on the interferometric signal autocorrelation matrix, the paper proposed the signal number estimation method based on information theoretic criteria, to distinguish Layover and Shadow from normal InSAR fields. The largest eigenvalue of the two-channel sample covariance matrix is exploited to early segment the shadow regions.

2. The Signal Model of Layover and Shadow

To pixel $P(k,l)$, the complex interferometric SAR image pairs are

$$\begin{aligned} y_0(k,l) &= \sum_{i=1}^{N_s} x_0^i(k,l)\mathrm{e}^{j\psi_i'(k,l)} + v_0(k,l) \\ y_1(k,l) &= \sum_{i=1}^{N_s} x_1^i(k,l)\mathrm{e}^{j\psi_i'(k,l)+j\psi_i(k,l)} + v_1(k,l) \end{aligned} \tag{1}$$

For homogeneous data, y_0, y_1 is a zero-mean, multidimensional, complex Gaussian pdf. Term x_0^i, x_1^i is the radar reflectivity, or texture, of the *i*-th source and it is modeled as an unknown deterministic parameter. N_S the number of sources, i.e. the number of terrain patches with different elevation angles in the layover areas. $\psi_i(k,l)$ is an unknown deterministic parameter representing the interferometric phase for the *i*-th terrain patch. v_0, v_1 is additive complex Gaussian white noise. Through channel equalization, the two channel SAR images power is almost equal. The interferometric signal can be expressed as

$$z(k,l) = A_z(k,l)\mathrm{e}^{j\psi_z(k,l)} = y_0(k,l)y_1^*(k,l) = \sum_{i=1}^{N_s} x_0^i(k,l)\left(x_1^i(k,l)\right)^* \mathrm{e}^{j\psi_i(k,l)} + v_0(k,l)v_1^*(k,l) + C(k,l) \tag{2}$$

In (22), A_z, ψ_z are the interferometric amplitude and phase, $C(k,l)$ is the cross term. The samples around pixel $P(k,l)$ can be used to reduce the phase estimation error. If the spatial averaging number is large enough, $C(k,l)$ is close to zero.

3. Layover and Shadow detection based on the covariance matrix

3.1. The interferometric signal covariance matrix

In [5]、[6], in the normal interferometric area, the phase ψ_z can be expressed as

$$\psi_z = \psi + \psi_v \tag{3}$$

Where ψ_z is the measured value, ψ_i is the phase without noise, and ψ_v represents a zero-mean noise with standard deviation σ_v . ψ_v is assumed to be an independent random variable. In [5]、[6], the interferogram is sub-divided into windows where the terrain is considered as a constant slope. In other words, signal in the window contains only one dominant frequency and can be modeled by a 2-D complex sine wave. In a filtering window W centered on sample $P(k,l)$,

$$z(k,l) = A_z(k,l)\mathrm{e}^{j2\pi(kf_x+lf_y)+j\psi_0(k,l)+j\psi_v(k,l)} \tag{4}$$

Where (m,n) refer to the samples in W, (f_x, f_y) is the 2-D local frequency of the interferometric fringe at pixel $P(k,l)$, and ψ_0 is the residual constant phase. In the layover areas, the signal model in (44) can be modified to (55).

$$z(k,l) = \sum_{i=1}^{N_s} A_z^i(k,l)\mathrm{e}^{j2\pi(kf_x^i+lf_y^i)+j\psi_0^i(k,l)+j\psi_v^i(k,l)} \tag{5}$$

According to (55), the interferometric signal is combined with Ns 2-D complex sine wave with different frequency. The length and shape of filtering window W can selected according to the fringe frequency. In this paper, the square window as M×M, where M=5, is used as an example to show the processing flow to the interferometric signal covariance matrix. As shown in the figure 1, the interferometric signal in the widow W (5×5) can be rearranged to 25-dimensional complex vectors $\vec{Z}_p$. The vector $\vec{Z}_p$ is defined as

$$\bar{Z}_P = \left[z(k-1,l-1), z(k-1,l), \ldots . z(k,l), z(k,l+1), \ldots . z(k+1,l+1) \right]^T \tag{6}$$

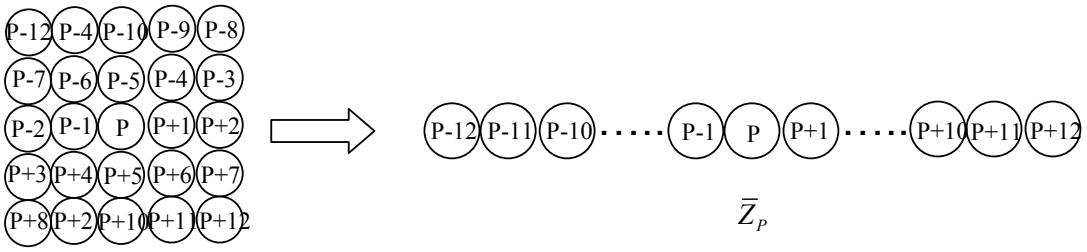

Figure 1. The vector $\bar{Z}_p$ rearranged from pixel P and its neighborhood pixel

The interferometric signal covariance matrix is

$$R = E\left[\bar{Z}_P \bullet \bar{Z}_P^H \right] \tag{7}$$

Where $(\bullet)^H$ denotes the Hermitian transpose operator. The eigen-decomposition of R in (7) yields

$$R = U \Sigma U^H \tag{8}$$

Σ is diagonally matrix, whose eigenvalue $\lambda_1 \geq \lambda_2 \cdots\cdots \geq \lambda_{M^2}$ and U is the corresponding eigenvectors. According to the signal model in (44) and the character of matrix eigen-decomposition, interferometric signal is sinusoidal signal. The largest eigenvalue λ_1 in Σ is signal eigenvalue. The other $M^2 - 1$ eigenvalues are the noise eigenvalues. In the layover areas, the echo from different areas decorrelated from each other, and the corresponding interferometric signal also decorrelated. The p large eigenvalues (EVs) in Σ are signal eigenvalues and the other $M^2 - N_s$ small eigenvalues are noise eigenvalues. In shadow areas, the interferometric signal is thermal noise. In the ideal case, the M^2 eigenvalues for matrix R is almost equal to each other, which all are noise eigenvalues.

To the normal interferometric phase areas, we analysis the element $r(u,v)$, $u,v = 1,\ldots,M^2$, which is in the matrix R.

$$\begin{aligned} r(u,v) &= E\left[z(m,n) \bullet z^*(m',n') \right] \\ &= E\left[A_z(m,n) \bullet A_z(m',n') \bullet \mathrm{e}^{j\{\psi(m,n) - \psi(m',n') + \psi_v(m,n) - \psi_v(m',n')\}} \right] \\ &= E\left[A_z(m,n) \bullet A_z(m',n') \right] \bullet E\left[\mathrm{e}^{j\{\psi(m,n) - \psi(m',n') + \psi_v(m,n) - \psi_v(m',n')\}} \right] \end{aligned} \tag{9}$$

In (99), m,n are the m_{th}, n_{th} elements in vector $\bar{Z}_P$, $m' = m - u$, $n' = n - v$. The first item in (99) is interferometric amplitude, which can be seen equal to each other.

$$P_A = E\left[A_z(m,n) \bullet A_z(m',n') \right] = E\left[A_z(m,n) \right] \bullet E\left[A_z(m',n') \right] \tag{10}$$

According to [5]、[6], the speckle noise decorrelations can be modeled as 2-D triangular-shaped spatial autocorrelation sequence.

$$E\left[\mathrm{e}^{j\{\psi_v(m,n) - \psi_v(m',n')\}} \right] = \begin{cases} 1 & u = v \\ K & u \neq v \end{cases} \qquad 0 \leq K \leq 1 \tag{11}$$

When the interferometric phase don't contain noise, K=1. On the other hand, when the signal are uncorrelated from each other, K=1. Then (99) can be written as

$$r(u,v) = E\left[A_z(m,n) \bullet A_z(m',n') \right] \bullet \mathrm{e}^{j2\pi(uf_x + vf_y)} \bullet \left(K + (1-K)\delta_{u,v} \right) \tag{12}$$

$\delta_{u,v}$ is Kronecker-Delta function. The interferometric signal covariance matrix in (88), can be expressed as

$$R = P_A \bullet R_s \odot \begin{bmatrix} 1 & K & \cdots & K \\ K & 1 & \cdots & K \\ \vdots & \vdots & \ddots & \vdots \\ K & K & \cdots & 1 \end{bmatrix} = P_A\left(K \bullet R_s + (1-K)I\right) = P_A\left(K \bullet \vec{a}_s \vec{a}_s^{H} + (1-K)I\right) \tag{13}$$

Where $\odot$ is the Shur-Hadamard product and I is an unit diagonally matrix. $\vec{a}_s$ is the signal steering vector.

$$\vec{a}_s = [1, e^{j2\pi f_x^i}, \ldots, e^{j2\pi(M-1)f_x}, \ldots, e^{j2\pi f_y}, e^{j2\pi(f_y+f_x)}, \ldots, e^{j2\pi\left[f_y+(M-1)f_x\right]}, \ldots, e^{j2\pi\left[(M-1)f_y+(M-1)f_x\right]}]^T \tag{14}$$

The speckle noise decorrelations can be modeled as 2-D covariance matrix tapering of the original interferometric signal matrix, which increases the leakage of signal power into the noise subspace (or EVs dispersion). After matrix eigen-decomposition, the eigenvalues sequence $\lambda_1, \lambda_2 \ldots \lambda_{M^2}$.

$$\lambda_1 = P_A\left(M^2 K + 1 - K\right) \tag{15}$$

Other $M^2 - 1$ eigenvalues are equal to $P_A \bullet K$. In the layover areas, the element $r(u,v)$ in (99) can be modified to

$$r(u,v) = \sum_{i=1}^{Ns} E\left[A_z(m,n) \bullet A_z(m',n')\right] \bullet E\left\{e^{j\left[\psi^i(m,n) - \psi^i(m',n') + \psi_v^i(m,n) - \psi_v^i(m',n')\right]}\right\} \tag{16}$$

And (1313) can be modified to

$$R = \sum_{i=1}^{N_s} P_A^i\left[K_i \bullet R_s^i + (1-K_i)I\right] = \sum_{i=1}^{N_s} P_A^i\left[K_i \bullet \vec{a}_s^i \bullet \left(\vec{a}_s^i\right)^H + (1-K_i)I\right] \tag{17}$$

$\vec{a}_i$ is the signal steering vector from the *i*-th area. In the shadow areas, the signals y_0, y_1 decorrelate from each other entirely. The interferometric amplitude in (1212)、(1313) and the phase is pure noise.

3.2. Layover and Shadow detection based on interferometric signal covariance matrix

As proposed in section 3.1, layover and shadow detection can be transformed to detect the number of sources. A commonly used approach for model order selection is based on information theoretic criteria (ITC), in particular the Akaike information criterion (AIC), the minimum description length (MDL), and the efficient detection criteria (EDC). All these algorithms consist of minimizing a criterion over the hypothesized number m of signals that are detectable, for N_s = 0, 1, M^2−1.

For example, EDC is defined as following,

$$EDC(N_s) = L\left(M^2 - N_s\right)\ln\Lambda(N_s) + N_s\left(2M^2 - N_s\right) \bullet f(L) \tag{18}$$

Where $\Lambda(\bullet)$ denotes likelihood function, which is defined

$$\Lambda(N_s) = \frac{1}{M^2 - N_s} \sum_{i=N_s+1}^{M^2} \lambda_i \cdot \left(\prod_{i=N_s+1}^{M^2} \lambda_i\right)^{-\frac{1}{M-N_s}} \tag{19}$$

Where λ_i is the eigenvalue of sample covariance matrix $\hat{R}$. N_s is the number of eigenvalue. And, the corresponding AIC and MDL rules are defined as,

$$AIC(N_s) = 2L\left(M^2 - N_s\right)\ln\Lambda(N_s) + 2N_s\left(2M^2 - N_s\right) \tag{20}$$

The corresponding eigenvalue number estimation can be defined as

$$\dim\left(\hat{R}\right) = \min_{N_s = 0,1,\ldots,M^2-1} AIC(N_s) \tag{21}$$

Where $\dim(\bullet)$ is the number of dimensions for signal subspace, which is also the number of signals. MDL rule is exploited in the paper to estimate the signal number in the interferometric signal. When $N_s = 1$, the pixel is detected as normal interferometric areas. When $N_s > 1$, the pixel is detected as layover pixel. When $N_s = 0$, the pixel is detected as shadow pixel.

4. Simulated experiment results and analysis

Interferograms are generated from simulated complex SAR image pairs to analyze the performance of the proposed method. We use the method proposed in [9] to simulate X-band SAR raw signal pairs representing round hole plus flat. The depth of the hole is 439.6 meters. Satellite velocity V= 7.6 Km/s, orbit altitude H =514.66 Km, wavelength λ= 0.031 m, PRF= 3.21 KHz, antenna size (length × width) 8.8m×0.6m, satellite number is 2,chirp bandwidth BW= 90 MHz. The satellites fly on the HELIX formation, whose baseline is 1000 meters. The master satellite transmits/receive and other slave satellites only receive the radar echo.

The simulated area Digital Elevation Model (DEM) is shown in figure 2(a). Figure 2(b) is the master satellite SAR image. After image coregistration, the noisy topographic phase is shown in figure 2(c). From figure 2(c), we can see that the phase in shadow area is pure noise, normal InSAR area is flat earth phase, and many interferometric signals are added in the layover area which composed from several fields. Figure 2(d)-(f) show detection result of the shadow area, normal area and layover area, which only include zero or one. In figure 2(d)-(f), one is labeled as the area is right to the selected, otherwise zero is labeled. We can see that shadow area detection performance is well. Miss detection appeared in layover area and false alarm appeared in the normal area.

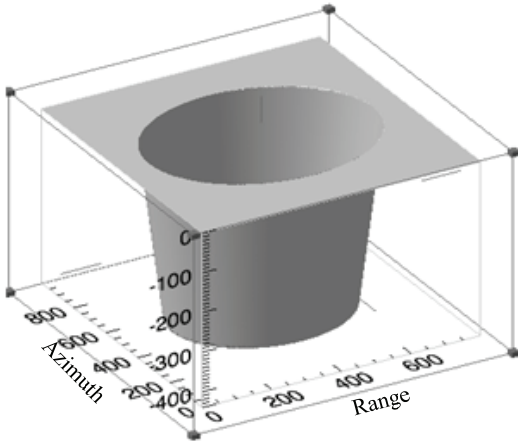

(a) DEM

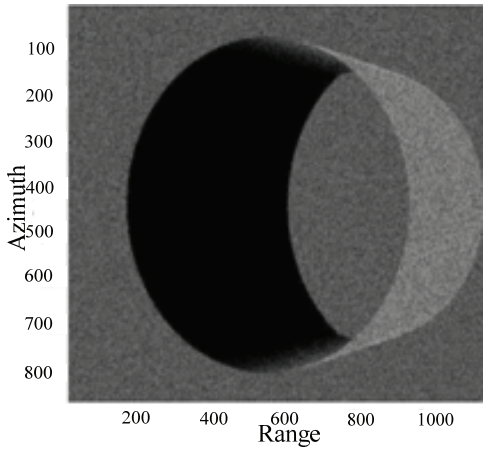

(b) Master satellite SAR image

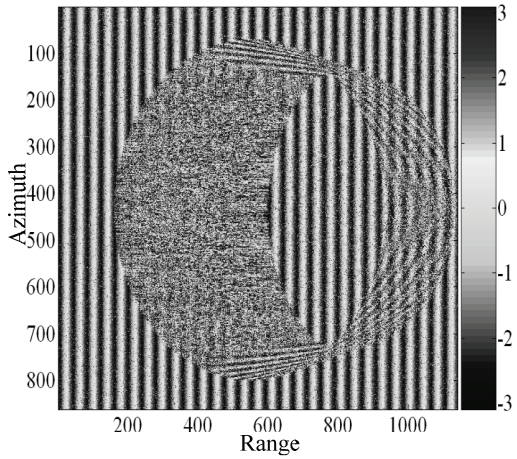

(c) Interferometric Phase

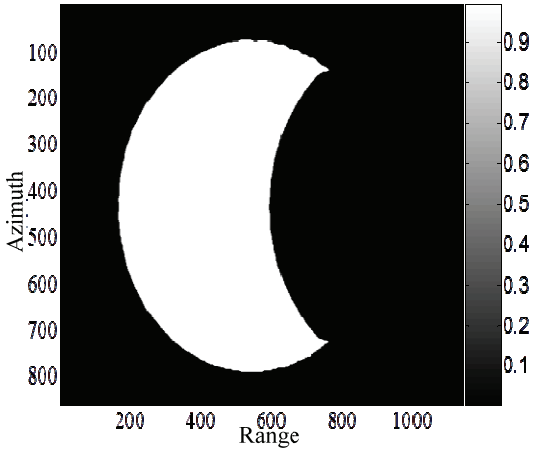

(d) Detection result of the shadow area

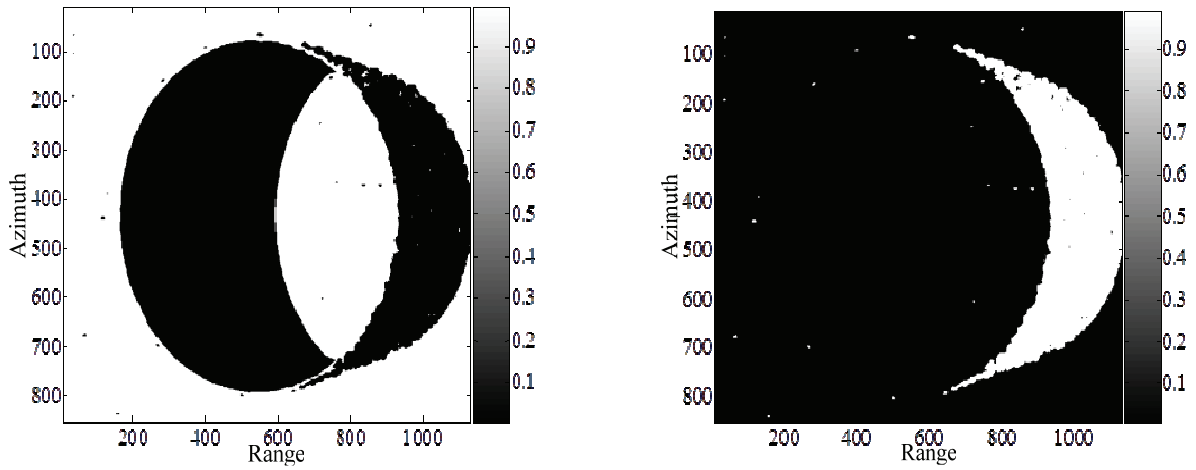

(e) Detection result of the normal area (f) Detection result of the layover area

Figure 2. Detection results

5. References

[1] M Eineder. Interferometric DEM Reconstruction of Alpine Areas-Experiences with SRTM Data and Improved Strategies for Future Missions 2005 *IEEE Trans. Geosci. Remote Sensing*. **37** 1317-1326.

[2] M Eineder and S. Suchandt, Recovering Radar Shadow to Improve Interferometric Phase Unwrapping and DEM Reconstruction. 2003 *IEEE Trans. Geosci. Remote Sensing*. **41** 2959-2962.

[3] F Gini, F Lombardini, M Montanari. Layover solution in multibaseline SAR interferometry. 2002 *IEEE Trans on Aerospace and Electronic Systems*. **38** 4.

[4] M Eineder, Nico Adam. A maximum-likelihood estimator to simultaneously unwrap, geocode, and fuse SAR interferograms from different viewing geometries into one digital elevation model. 2005 *IEEE Trans. Geosci. Remote Sensing*. **43** 24-36,.

[5] Bin Cai, Diannong Liang and Zhen Dong, A New Adaptive Multiresolution Noise-Filtering Approach for SAR Interferometric Phase Images. 2008 *IEEE Geosci. Remote Sens. Letters*, **5** 266-270.

[6] M Eineder, Efficient simulation of SAR interferogram of large areas and of rugged terrain, 2003 *IEEE Trans. Geosci. Remote Sensing*. **41** 1415-1427